Evaluating Environmental Weathering Effects on White Portland Cement using Hyperspectral Reflectance Analysis

Ishtiaq Ahmed[1], Umesh Kumar Sharma[1] , Pradeep Kumar Garg[1] , Aditya Kumar Thakur[1], Pritipadmaja[1]
[1]Department of Civil Engineering, Indian Institute of Technology Roorkee, Haridwar, India – ishtiaq_a@ce.iitr.ac.in, umesh.sharma@ce.iitr.ac.in, p.garg@ce.iitr.ac.in, aditya_kt@ce.iitr.ac.in, pritipadmaja@ce.iitr.ac.in.

Keywords: Hyperspectral Reflectance Analysis, White Portland Cement, Environmental Weathering, Surface Reflectance Dynamics, Cement Durability Monitoring.

Abstract

Cement is a primary binding material that plays a crucial role in construction. This study used hyperspectral reflectance analysis to investigate the spectral reflectance characteristics of White Portland Cement (WPC) exposed to environmental conditions. The observation was made over a 150-day period. The reflectance of cement samples was measured using a spectroradiometer that captures the reflectance value of 994 discrete wavelength range from 339.3 nm to 2516.8 nm. These data were processed to calculate differential and double differential curves. Statistical techniques like moving average and smooth spline interpolation were employed to remove local fluctuations and observe the changing trends in reflectance over time. The study results provide insight into the temporal changes in the surface properties of WPC. The analysis also revealed significant changes in reflectance over time. The mean reflectance decreased from 90.397 on Day 0 to 83.092 on Day 150, showing surface degradation with time. However, the standard deviation of the reflectance increased initially from 7.318 on Day 0 to 7.766 on Day 30, then stabilized at 6.763 by Day 120. It was further increased to 7.496 by Day 150. The differential and double differential curves also show significant variations. The differential reflectance attained its maximum value of 0.199 on Day 60, and the double differential reflected maximum changes at 0.031 on Day 60. These results highlight the dynamic interaction between WPC surfaces and various environmental factors. The observed decrease in reflectance over time suggests surface ageing and potential material degradation, as reduced reflectance may indicate increased porosity or surface roughness due to environmental exposure. Overall, this study can offer a valuable tool for assessing cement-based materials' long-term durability and performance in the construction industry.

1. Introduction

Concrete and mortar are essential construction materials. These materials are known for their durability, strength, and other important parameters that may affect the building's behaviour. These characteristics play a crucial role in ensuring the quality and integrity of building structures (Domone and Illston, 2018; Kolhe et al., 2024). The properties of concrete and mortar are significantly influenced by the quality and composition of cement used during preparation time. Cement directly affects materials' strength, workability, and durability (Dhir et al., 2004; Kurdowski, 2014; Thomas, 2013). The properties of various construction materials, such as cement and mortar, are continuously influenced by the complex interplay of various factors, environmental conditions, material composition, and manufacturing processes (Domone and Illston, 2018; Duggal, 2017; Habert et al., 2020). A thorough understanding of material properties is critical for ensuring the quality, durability, and safety of buildings and other structures.

The properties of building materials can be broadly classified as physical, mechanical, chemical, electrical, magnetic, and thermal (Duggal, 2017; Papadopoulos et al., 2006). Physical properties include properties such as density, porosity, and surface texture, which influence the material's weight and durability (Fernando et al., 2023; Kodur and Harmathy, 2016). Mechanical properties, such as compressive and tensile strength, determine the material's load-bearing capacity and resistance to deformation and external forces (Ashby and Jones, 2012; François et al., 1998). Chemical properties include reactivity and stability, influencing durability in aggressive environments (Fregert and Gruvberger, 1972; Pacheco-Torgal et al., 2012; Ruscher et al., 2011). Electrical and magnetic properties, though less important in construction, electrical and magnetic properties play a role in special applications, such as insulating or conductive materials. Further, thermal properties, including conductivity and resistance, are essential for understanding the material's behaviour under temperature variations. It is crucial for energy-efficient designs of buildings (Balaji et al., 2014; Bertolini et al., 2013; Carlsson et al., 2014; Hlaváčová, 2007; Honorio et al., 2020; Jiang et al., 2022; Joshaghani et al., 2018; Kumar and Sharma, 2024; Meukam et al., 2004; Mishra and Sharma, 2024; Papadakis et al., 1991).

White Portland Cement (WPC) is a specific type of cement with a bright colour due to its low content of iron oxide and its specific production process. WPC also has aesthetic value and high durability. It makes it suitable for use as an architectural element, ornamentation, and precast element. However, with time, environmental factors, particularly carbonation, exposure to moisture, and pollutant accumulation may cause changes in WPC's surface appearance and other characteristics. Quality assessment of cement samples has traditionally been done by conducting several tests on the sample and complying with internationally established standard procedures. Various tests are carried out to check the composition and other properties of a given cement sample. It includes fineness, consistency, setting time, or even compressive strength. These factors ensure that a certain cement meets the requirements and standards of construction. Such assessments are particularly important in establishing the potential use of cement in constructing several structural components (Opedal et al., 2018; Spragg et al., 2013; Standard, 2005, 2009).

Modern technologies for testing have increased efficiency and level of detail. Ultrasonic testing, for example, uses high-frequency sound waves to evaluate material integrity, density, and defects non-destructively, preserving sample usability (Karaiskos et al., 2015; Washer et al., 2004). X-ray tomography uses imaging to create detailed cross-sections, revealing internal features and defects for comprehensive material analysis without destructive sampling (du Plessis and Boshoff, 2019; Vicente et al., 2019). Further, Infrared Thermography also known as thermal imaging, captures infrared radiation to visualize heat distribution and variations in a structure using a thermal imaging camera (Sirca Jr and Adeli, 2018).

Remote sensing plays a crucial role in various fields, including disaster management, material identification, change detection, environmental monitoring, urban planning, agriculture, forestry, hydrology, and infrastructure assessment (Bhattacharjee and Garg, 2024; Gond et al., 2024; Grimaldi et al., 2020; Holmgren and Thuresson, 1998; Kokaly, 2012; Mondal and Paul, 2023; Pritipadmaja et al., 2023; Srivastava et al., 2025; Tang et al., 2024; Thakur et al., 2024, 2025; Vanama et al., 2020; Verma and Vijay, 2024; Ye et al., 2017). In material testing, it offers significant advantages over traditional testing methods as a non-destructive approach (Cavalli et al., 2011; El Masri and Rakha, 2020; Fan et al., 2020; Gagliardi et al., 2023). This technology enables efficient, multi-scale data collection and rapid analysis using high-speed computing, minimizing fieldwork. It captures diverse object information through various spectral wavelengths (Ahmed et al., 2024; Chang, 1999; Martínez et al., 2024; Shaban, 2013). Spectral reflectance acts as a unique signature for predicting composite materials' constituents and properties. Devices like radiometers, spectro-radiometers, NMR, and techniques like FTIR spectroscopy, provide detailed object analysis. (Brook and Ben-Dor, 2011; Roberts and Herold, 2004). Advanced methods enable precise analysis, improving understanding of material composition and behaviour. They offer researchers more accurate property assessments.

This study presents a comprehensive analysis of the spectral reflectance characteristics of WPC subjected to extended environmental exposure. The dynamic behaviour of change in reflectance with time is analysed. The intricate details of surface evolution are captured using advanced data processing techniques, including spline interpolation, filtering, and smoothing. Differential and double differential transformations further enhance the understanding of transitional phases and surface stabilization. The findings of this study provide valuable insights into the durability and performance of WPC in diverse environmental conditions. The results not only advance the understanding of material behaviour but also offer practical implications for assessing and predicting the long-term structural and aesthetic properties of cement-based materials, contributing to sustainable construction practices. Further, this study provides insights into material durability by analysing changes in surface reflectance over time, which can be linked to microstructural changes in the cement. However, since all experiments were conducted under controlled conditions, the impact of diverse environmental factors remains unexplored and is suggested for future studies.

2. Methodology

2.1 Experimental Setup

White Portland Cement (WPC) is a high-quality, finely ground cement with a white colour appearance. It is primarily composed of calcium oxide (CaO), silicon dioxide (SiO_2), and aluminium oxide (Al_2O_3) (Table 1). It is used in applications requiring aesthetic value enhancement, such as architectural finishes, decorative concrete, and precast elements. WPC has a lower iron oxide (Fe_2O_3) content compared to Ordinary Portland Cement (OPC), which contributes to its white colour. Additionally, it has a slightly higher concentration of magnesium oxide (MgO). It enhances its durability in certain environmental conditions.

Table 1. Chemical Composition of White Portland Cement (WPC)

Chemical Components	Weight (%)
Silicon Dioxide (SiO_2)	21–25
Aluminum Oxide (Al_2O_3)	0.86–0.92
Iron Oxide (Fe_2O_3)	0.26–0.30
Calcium Oxide (CaO)	60–69
Magnesium Oxide (MgO)	1.5–1.9
Sulfur Trioxide (SO_3)	2.9–3.3

Hyperspectral imaging allows for a detailed spectral analysis of surface changes, providing more information than conventional imaging techniques. By measuring reflectance across a broad range of wavelengths, we can detect subtle spectral variations associated with surface degradation. Figure 1 represents the spectroradiometer and WPC sample for the reflectance analysis. The spectroradiometer was configured according to the experimental requirements and calibrated using a reference white plate. It ensures accurate reflectance measurements. Calibration was performed by calculating the ratio of the target scan to the reference scan. Spectral readings for the three cement samples were then recorded, with 10 measurements taken for each sample. The data was stored in the instrument in SIG file format and subsequently downloaded using the instrument's PC Data Acquisition Software installed on a computer.

Figure 1. A spectroradiometer and a sample of WPC were used for testing.

2.2 Processing

The reflectance values of 994 discrete data ranging from wavelength 339.3nm to 2516.8nm were taken using a spectroradiometer. Capturing reflectance over a wide wavelength range enables comprehensive material characterization, aiding in the identification of surface properties, composition, and spectral signatures. Further, the reflectance differential was calculated for every data point using Equation 1. Calculating the reflectance differential at each data point enhances the detection of subtle spectral variations.

$$\left(\frac{\Delta \boldsymbol{R}}{\Delta \lambda}\right)_{\boldsymbol{n}} = \frac{\left(\frac{\boldsymbol{R_n}-\boldsymbol{R_{n-1}}}{\boldsymbol{\lambda_n}-\boldsymbol{\lambda_{n-1}}} + \frac{\boldsymbol{R_{n+1}}-\boldsymbol{R_n}}{\boldsymbol{\lambda_{n+1}}-\boldsymbol{\lambda_n}}\right)}{\mathbf{2}} \qquad (1)$$

Where $\boldsymbol{R_n}$ and $\left(\frac{\Delta \boldsymbol{R}}{\Delta \lambda}\right)_{\boldsymbol{n}}$ represents values of reflectance and its differential, respectively, at $\boldsymbol{n_{th}}$ data point. Further, the double differential $\left(\frac{\Delta\left(\frac{\Delta \boldsymbol{R}}{\Delta \lambda}\right)}{\Delta \lambda}\right)_{\boldsymbol{n}}$ were calculated using Equation 2. Computing the double differential of reflectance helps identify rapid spectral variations, enhancing feature extraction, and edge detection. The plot for reflectance, its differential and double differential are shown in Figure 2.

$$\left(\frac{\Delta\left(\frac{\Delta \boldsymbol{R}}{\Delta \lambda}\right)}{\Delta \lambda}\right)_{\boldsymbol{n}} = \frac{\left(\frac{\left(\frac{\Delta \boldsymbol{R}}{\Delta \lambda}\right)_{\boldsymbol{n}}-\left(\frac{\Delta \boldsymbol{R}}{\Delta \lambda}\right)_{\boldsymbol{n-1}}}{\boldsymbol{\lambda_n}-\boldsymbol{\lambda_{n-1}}} + \frac{\left(\frac{\Delta \boldsymbol{R}}{\Delta \lambda}\right)_{\boldsymbol{n+1}}-\left(\frac{\Delta \boldsymbol{R}}{\Delta \lambda}\right)_{\boldsymbol{n}}}{\boldsymbol{\lambda_{n+1}}-\boldsymbol{\lambda_n}}\right)}{\mathbf{2}} \qquad (2)$$

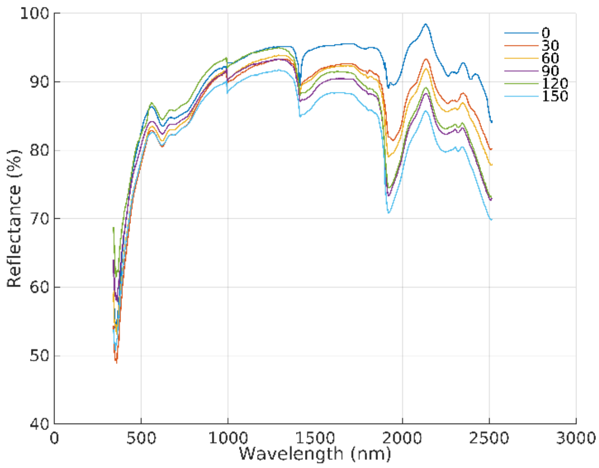

(a)

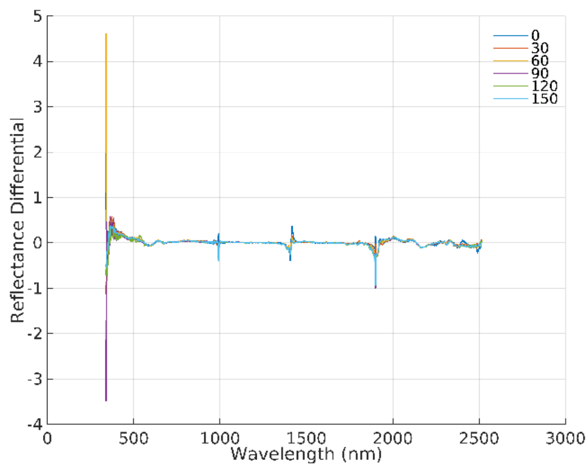

(b)

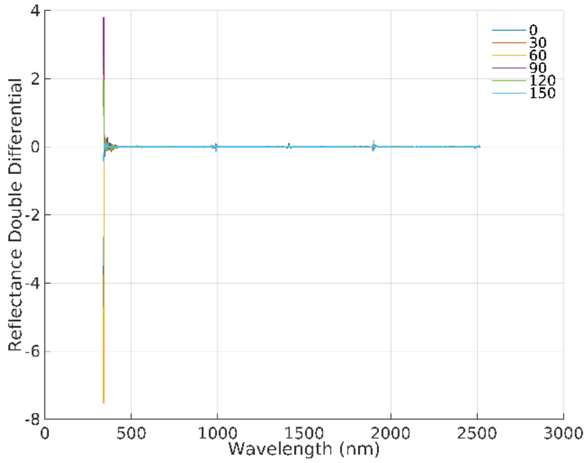

(c)

Figure 2. Original (a) Reflectance curve, (b) Reflectance differential curve, and (c) Reflectance double differential curve of WPC exposed to the environment for different days.

2.3 Curve Smoothening

The process of smoothening involved analyzing reflectance, as well as its differential and curvature data, using multiple step-by-step processes. It includes spline interpolation, filtering, and re-smoothening using the moving average method. First, the reflectance values were interpolated using a cubic spline approach (Equation 3) to create smooth, continuous curves across 1000 equally spaced wavelength points over the domain.

$$\boldsymbol{R_{interp}(\lambda) = \sum_{i=1}^{n} N_i(\lambda) \,.\, R_i} \qquad (3)$$

Where $R_{interp}(\lambda)$ is the interpolated reflectance at wavelength λ, $N_i(\lambda)$ is basis spline function and R_i is the original reflectance data points. Further mean (μ) and standandard deviation (σ) were calculated using Equation 4 and Equation 5, respectively, allowing the removal of outliers that deviated beyond two standard deviations from the mean.

$$\mu = \frac{1}{n}\sum_{i=1}^{n} R_{interp}(\lambda_i) \qquad (4)$$

$$\sigma = \left(\frac{1}{n}\sum_{i=1}^{n}(R_{interp}(\lambda_i) - \mu)\right)^{\frac{1}{2}} \qquad (5)$$

Following this, a moving average with a 100 nm window was applied to further smooth the data and reduce high-frequency noise, ensuring the retention of essential curve features (Equation 6).

$$\hat{R}(\lambda_i) = \frac{1}{n_w}\sum_{\lambda_j \in W(\lambda_i)} R_{valid}(\lambda_j) \qquad (6)$$

Where $W(\lambda_i)$ is the window of wavelengths within ±50 nm of λ_i, n_w is the number of points within the window, and $\hat{R}(\lambda_i)$ is the smoothed reflectance. The smoothed curves were plotted for each angle, with the wavelength on the x-axis and the corresponding reflectance on the y-axis, enabling a comparative visual analysis.

Key statistical metrics were computed to support quantitative assessments, including mean, standard deviation, and reflectance range. The same steps were repeated to obtain the smooth curve for differential and double differential reflectance. The differential and double differential calculations help in identifying subtle trends and variations in spectral data. These measures enhance the ability to detect nonlinear changes in reflectance, which may be linked to material ageing and degradation patterns.

3. Results and Discussions

3.1. General Curve Analysis

Table 2. Statistical parameters of processed Reflectance curve of WPC exposed to the environment for different days.

Days	Mean	Standard Deviation	Max	Min
0	90.397	7.318	97.260	79.010
30	86.799	7.766	93.239	74.739
60	86.616	7.291	93.766	75.172
90	85.254	6.828	93.200	73.658
120	86.632	6.763	94.842	74.156
150	83.092	7.496	91.582	70.795

The statistical analysis of the processed reflectance curves (Figure 3) of White Portland Cement (WPC) exposed to environmental conditions over different time intervals reveals significant trends (Table 2). Initially, the mean reflectance value is highest at 90.397 (Day 0), indicating the cement's pristine state with a smooth and unaltered surface. Over time, the mean reflectance gradually decreases, reaching 83.092 by Day 150. This decline suggests progressive surface changes due to environmental factors such as dust deposition, surface carbonation, or hydration processes, which alter the optical properties of the cement. These changes are consistent with the effects of carbonation, where calcium hydroxide reacts with atmospheric CO_2, forming calcium carbonate and reducing surface reflectivity. The standard deviation starts at 7.318 (Day 0), increases to 7.766 (Day 30), and then stabilizes around 6.763 by Day 120 before slightly rising again. This pattern may indicate an initial increase in surface variability caused by uneven environmental effects, followed by a period of stabilization as hydration and weathering processes proceed uniformly.

The maximum and minimum reflectance values also gradually decrease over time. The reflectance range narrows significantly over time, highlighting the decrement of band-wise reflectance variation over time. This trend underscores the combined impact of surface weathering and contaminant accumulation, which reduce surface brightness and smooth out irregularities. However, the mean reflectance value at Day 120 (86.632) slightly increases compared to earlier stages, suggesting potential surface densification or hardening due to ongoing hydration reactions. Moreover, the subsequent decline by Day 150 indicates continued degradation, possibly due to further exposure to pollutants or moisture. The observed changes highlight the dynamic interplay between environmental exposure and the surface properties of WPC, emphasizing the importance of monitoring such variations for assessing material durability, structural performance, and long-term aesthetic implications in construction and infrastructure applications.

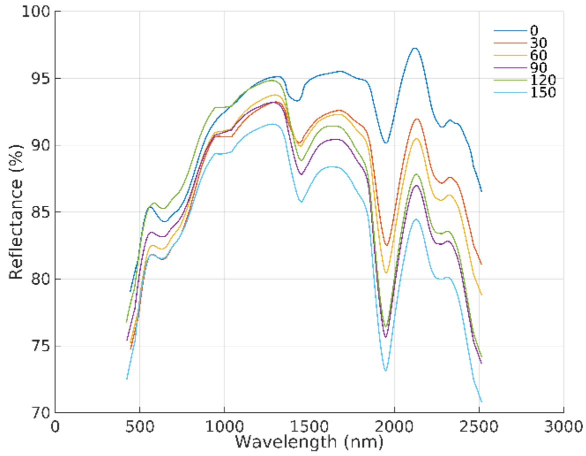

Figure 3. Processed reflectance curve of WPC was exposed to the environment for different days.

3.2. Differential Curve Analysis

Table 3. Statistical parameters of processed Reflectance differential curve of WPC exposed to the environment for different days.

Days	Mean	Standard Deviation	Max	Min
0	0.015	0.105	0.166	-0.086
30	0.012	0.093	0.164	-0.062
60	0.014	0.171	0.199	-0.099
90	0.002	0.145	0.164	-0.111
120	0.002	0.09	0.138	-0.075
150	0.007	0.091	0.161	-0.074

The statistical parameters of the processed reflectance differential curves (Figure 4) for White Portland Cement (WPC) exposed to environmental conditions reveal subtle but significant insights into surface changes over time (Table 3). The mean values of the differential curves remain close to zero across all exposure durations, indicating minimal net variation in reflectance across wavelengths. This consistency suggests that the primary surface alterations are uniform across the spectral range, likely driven by physical and chemical processes such as carbonation, hydration, and pollutant deposition. However, the standard deviation fluctuates, peaking at 0.171 on Day 60 and then stabilizing to lower values (0.09–0.145) by Day 150. This trend implies an initial phase of increased surface heterogeneity, potentially due to the uneven progression of environmental effects, followed by stabilization as the surface undergoes more uniform changes.

The maximum and minimum values of the reflectance differential curves also exhibit variability, with the widest range occurring at Day 60 (0.199 to -0.099). This phase of pronounced variation may correspond to transitional surface changes, such as the partial removal of contaminants or hydration by-products under environmental exposure. By Day 120, the range narrows considerably, indicating a stabilization of surface properties, possibly due to the dominance of carbonation or surface hardening effects. However, a slight increase in maximum reflectance values at Day 150 suggests that additional factors, such as localized pollutant removal or drying effects, might influence surface reflectivity. These findings highlight the dynamic interplay between environmental exposure and material surface evolution, with implications for assessing the durability and performance of cement-based materials over time.

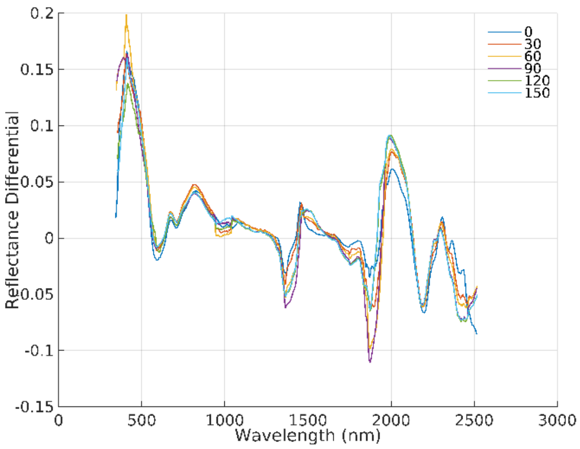

Figure 4. Processed Reflectance differential curve of WPC exposed to the environment for different days.

3.3. Double Differential Curve Analysis

Table 4. Statistical parameters of processed Reflectance double differential curve of WPC exposed to the environment for different days.

Days	Mean	Standard Deviation	Max	Min
0	-0.007	0.189	0.013	-0.004
30	0.005	0.108	0.013	-0.005
60	-0.009	0.243	0.031	-0.005
90	0.005	0.129	0.01	-0.009
120	0.003	0.064	0.012	-0.005
150	-0.001	0.018	0.005	-0.004

The statistical analysis of the processed reflectance double differential curves (Figure 5) for White Portland Cement (WPC) exposed to environmental conditions highlights the nuanced changes in spectral reflectance over time (Table 4). The mean values of the double differential curves are minimal, ranging between -0.009 and 0.005, indicating that the higher-order changes in reflectance are subtle and primarily represent minor variations in surface properties. Notably, the standard deviation values decrease progressively over the exposure period, starting from a peak of 0.243 on Day 60 and reducing significantly to 0.018 by Day 150. This trend suggests an initial period of pronounced variability in higher-order reflectance changes, potentially due to active surface transformations such as carbonation, hydration, or pollutant deposition. The subsequent reduction in variability reflects a stabilization phase, where the surface achieves a more uniform and less reactive state.

The extreme (maximum and minimum) values of the double differential curves underscore the dynamic behaviour of change across different ranges of wavelengths. On Day 60, the range is relatively broad, with a maximum of 0.031 and a minimum of -0.005, indicating significant surface-process heterogeneity. However, by Day 150, the range narrows considerably (maximum of 0.005 and minimum of -0.004), emphasizing that the surface transitions to a stable, less dynamic phase. This stabilization may result from the dominance of long-term environmental effects such as carbonation and surface hardening, which homogenize the reflectance characteristics. These findings provide a detailed understanding of the temporal evolution of WPC surfaces, with implications for predicting durability and assessing environmental exposure effects on cementitious materials.

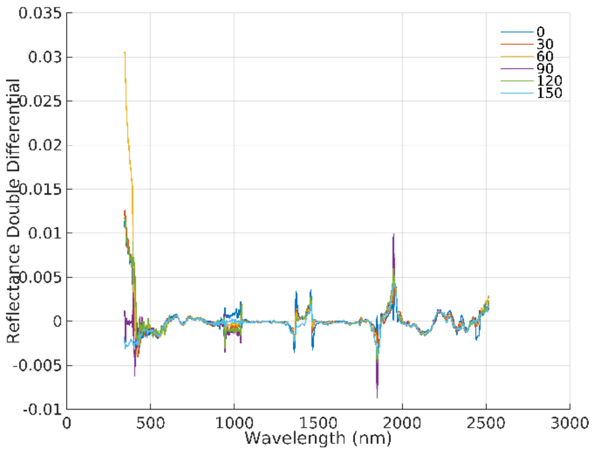

Figure 5. Processed Reflectance double differential curve of WPC exposed to the environment for different days.

4. Conclusion

This study provides a comprehensive analysis of the spectral reflectance characteristics of White Portland Cement (WPC) exposed to environmental conditions over an extended period. The processed value of reflectance and its differential and double differential reveal significant trends. It illustrates the progressive changes in WPC's optical and surface properties. Initially, the pristine surface of WPC exhibited high reflectance values. It gradually decreases over time due to environmental factors such as carbonation, hydration, and pollutant deposition. The differential and double differential curves further highlighted transitional surface phases. Analysis of the curve shows increased heterogeneity in the early stages of exposure, followed by stabilization as the surface properties became more uniform.

The smoothing and statistical techniques used in the data processing enable clearer insights into the temporal evolution of WPC surfaces. The findings emphasize the dynamic interplay between environmental entities and material properties. It demarcates the importance of spectral reflectance analysis as a non-destructive method for assessing material performance and durability. The results of the study have practical implications for the construction industry. It can be used to predict cementitious materials' long-term aesthetic and structural behaviour in diverse environmental conditions. The methodology and findings can be extended to other cement types and environmental contexts. It can provide a robust framework for durability assessment and sustainable material development.

https://doi.org/10.5194/isprs-archives-XLVIII-G-2025-79-2025

Acknowledgement

The authors thank to the Indian Institute of Technology Roorkee for providing the environment for conducting this research work. We also extend our thanks to all those who contributed directly or indirectly to the successful completion of this work.

References

Ahmed, I., Sharma, U.K., Garg, P.K., Thakur, A.K., 2024. Analysis of Cement properties using Hyperspectral Remote Sensing methods. ISPRS Ann. Photogramm. Remote Sens. Spat. Inf. Sci. 10, 15–20.

Ashby, M.F., Jones, D.R.H., 2012. Engineering materials 1: an introduction to properties, applications and design. Elsevier.

Balaji, N.C., Mani, M., Reddy, B.V.V., 2014. Discerning heat transfer in building materials. Energy Procedia 54, 654–668.

Bertolini, L., Carsana, M., Daniotti, B., Marra, E., 2013. Environmental factors affecting corrosion of steel inserts in ancient masonry. Durab. Build. Mater. Components 229–252.

Bhattacharjee, S., Garg, R.D., 2024. Estimation of sea ice drift and concentration during melt season using C-band dual-polarimetric Sentinel-1 data. Remote Sens. Appl. Soc. Environ. 33, 101104.

Brook, A., Ben-Dor, E., 2011. Reflectance spectroscopy as a tool to assess the quality of concrete in situ.

Carlsson, L.A., Adams, D.F., Pipes, R.B., 2014. Experimental characterization of advanced composite materials. CRC press.

Cavalli, R.M., Bassani, C., Palombo, A., Pascucci, S., Pignatti, S., Santini, F., 2011. Exploitation of hyperspectral data for infrastructures status assessment: Preliminary results of the istimes test bed, in: 2011 3rd Workshop on Hyperspectral Image and Signal Processing: Evolution in Remote Sensing (WHISPERS). IEEE, pp. 1–4.

Chang, C.-I., 1999. Spectral information divergence for hyperspectral image analysis, in: IEEE 1999 International Geoscience and Remote Sensing Symposium. IGARSS'99 (Cat. No. 99CH36293). IEEE, pp. 509–511.

Dhir, R.K., McCarthy, M.J., Zhou, S., Tittle, P.A.J., 2004. Role of cement content in specifications for concrete durability: cement type influences. Proc. Inst. Civ. Eng. Build. 157, 113–127.

Domone, P., Illston, J., 2018. Construction materials: their nature and behaviour. CRC press.

du Plessis, A., Boshoff, W.P., 2019. A review of X-ray computed tomography of concrete and asphalt construction materials. Constr. Build. Mater. 199, 637–651.

Duggal, S.K., 2017. Building materials. Routledge.

El Masri, Y., Rakha, T., 2020. A scoping review of non-destructive testing (NDT) techniques in building performance diagnostic inspections. Constr. Build. Mater. 265, 120542.

Fan, L., Fan, M., Alhaj, A., Chen, G., Ma, H., 2020. Hyperspectral imaging features for mortar classification and compressive strength assessment. Constr. Build. Mater. 251, 118935.

Fernando, S., Gunasekara, C., Law, D.W., Nasvi, M.C.M., Setunge, S., Dissanayake, R., 2023. Assessment of long term durability properties of blended fly ash-Rice husk ash alkali activated concrete. Constr. Build. Mater. 369, 130449.

François, D., Pineau, A., Zaoui, A., 1998. Mechanical behaviour of materials. Springer.

Fregert, S., Gruvberger, B., 1972. Chemical properties of cement. Berufsdermatosen 20, 238–248.

Gagliardi, V., Tosti, F., Bianchini Ciampoli, L., Battagliere, M.L., D'Amato, L., Alani, A.M., Benedetto, A., 2023. Satellite remote sensing and non-destructive testing methods for transport infrastructure monitoring: Advances, challenges and perspectives. Remote Sens. 15, 418.

Gond, A.K., Jamal, A., Verma, T., 2024. Spatio-temporal trend analysis of air pollutants during COVID-19 over Korba district, Chhattisgarh (India) using Google Earth Engine. Remote Sens. Appl. Soc. Environ. 33, 101143. https://doi.org/10.1016/j.rsase.2024.101143

Grimaldi, S., Xu, J., Li, Y., Pauwels, V.R.N., Walker, J.P., 2020. Flood mapping under vegetation using single SAR acquisitions. Remote Sens. Environ. 237, 111582.

Habert, G., Miller, S.A., John, V.M., Provis, J.L., Favier, A., Horvath, A., Scrivener, K.L., 2020. Environmental impacts and decarbonization strategies in the cement and concrete industries. Nat. Rev. Earth Environ. 1, 559–573.

Hlaváčová, Z., 2007. Electrical properties of some building materials. Res. Teach. Phys. Context Univ. Educ. Proc. Sci. Work. 134–140.

Holmgren, P., Thuresson, T., 1998. Satellite remote sensing for forestry planning—a review. Scand. J. For. Res. 13, 90–110.

Honorio, T., Carasek, H., Cascudo, O., 2020. Electrical properties of cement-based materials: Multiscale modeling and quantification of the variability. Constr. Build. Mater. 245, 118461.

Jiang, L., Pettitt, T.R., Buenfeld, N., Smith, S.R., 2022. A critical review of the physiological, ecological, physical and chemical factors influencing the microbial degradation of concrete by fungi. Build. Environ. 214, 108925.

Joshaghani, A., Balapour, M., Ramezanianpour, A.A., 2018. Effect of controlled environmental conditions on mechanical, microstructural and durability properties of cement mortar. Constr. Build. Mater. 164, 134–149.

Karaiskos, G., Deraemaeker, A., Aggelis, D.G., Van Hemelrijck, D., 2015. Monitoring of concrete structures using the ultrasonic pulse velocity method. Smart Mater. Struct. 24, 113001.

Kodur, V.K.R., Harmathy, T.Z., 2016. Properties of building materials. SFPE Handb. fire Prot. Eng. 277–324.

Kokaly, R.F., 2012. Spectroscopic remote sensing for material identification, vegetation characterization, and mapping, in: Algorithms and Technologies for Multispectral, Hyperspectral, and Ultraspectral Imagery XVIII. SPIE, pp. 311–322.

Kolhe, A.R., Thorat, V.S., Gorde, P.J., Chandgude, M.S.E., 2024. TEXT BOOK OF BUILDING CONSTRUCTION AND CONSTRUCTION MATERIALS. Academic Guru Publishing House.

Kumar, W., Sharma, U.K., 2024. Post-fire mechanical properties of low-alloyed YSt-355-FR (126% Mo) fire-resistant steel. J. Constr. Steel Res. 223, 109064.

Kurdowski, W., 2014. Concrete properties. Cem. Concr. Chem. 369–532.

Martínez, D.E.V., Saba, M., Gil, L.K.T., 2024. Assessment of asbestos-cement roof distribution and prioritized intervention approaches through hyperspectral imaging. Heliyon 10.

Meukam, P., Jannot, Y., Noumowe, A., Kofane, T.C., 2004. Thermo physical characteristics of economical building materials. Constr. Build. Mater. 18, 437–443.

Mishra, L., Sharma, U.K., 2024. Behaviour of deteriorated reinforced concrete columns under elevated temperatures. Fire Technol. 60, 1569–1607.

Mondal, A., Paul, P.K., 2023. Monitoring of groundwater generated land subsidence by persistent scatterer analysis–A case study of the Kolkata Municipal Corporation (KMC), West Bengal. J. Earth Syst. Sci. 132, 181.

Opedal, N., Corina, A.N., Vrålstad, T., 2018. Laboratory test on cement plug integrity, in: International Conference on Offshore Mechanics and Arctic Engineering. American Society of Mechanical Engineers, p. V008T11A071.

Pacheco-Torgal, F., Jalali, S., Fucic, A., 2012. Toxicity of building materials. Elsevier.

Papadakis, V., Vayenas, C., Fardis, M., 1991. Physical and chemical characteristics affecting the durability of concrete. ACI Mater. J. 88, 186–196.

Papadopoulos, A.N., Ntalos, G.A., Kakaras, I., 2006. Mechanical and physical properties of cement-bonded OSB. Holz als Roh-und Werkst. 64, 517–518.

Pritipadmaja, Garg, R.D., Sharma, A.K., 2023. Assessing the cooling effect of blue-green spaces: implications for Urban Heat Island mitigation. Water 15, 2983.

Roberts, D.A., Herold, M., 2004. Imaging spectrometry of urban materials. Infrared Spectrosc. Geochemistry, Explor. Remote Sensing, Miner. Assoc. Canada, Short Course Ser. 33, 155–181.

Ruscher, C.H., Mielcarek, E.M., Wongpa, J., Jaturapitakkul, C., Jirasit, F., Lohaus, L., 2011. Silicate-, aluminosilicate and calciumsilicate gels for building materials: Chemical and mechanical properties during ageing. Eur. J. Mineral. 23, 111–124.

Shaban, A., 2013. Determination of concrete properties using hyperspectral imaging technology: A review. Sci. J. Phys. 2013.

Sirca Jr, G.F., Adeli, H., 2018. Infrared thermography for detecting defects in concrete structures. J. Civ. Eng. Manag. 24, 508–515.

Spragg, R., Bu, Y., Snyder, K., Bentz, D., Weiss, J., 2013. Electrical testing of cement-based materials: Role of testing techniques, sample conditioning, and accelerated curing.

Srivastava, A., Thakur, A.K., Garg, R.D., 2025. An Assessment of the Spatiotemporal Dynamics and Seasonal Trends in NO_2 Concentrations Across India Using Advanced Statistical Analysis. Remote Sens. Appl. Soc. Environ. 101490.

Standard, B., 2005. Methods of testing cement. Determ. strength.

Standard, E., 2009. Methods of testing cement-Part 1: Determination of strength. Turkish Stand. Institute, Ankara, Turkey.

Tang, T., Zhang, L., Zhu, H., Ye, X., Fan, D., Li, X., Tong, H., Li, S., 2024. Quantifying Urban Daily Nitrogen Oxide Emissions from Satellite Observations. Atmosphere (Basel). 15, 1–12. https://doi.org/10.3390/atmos15040508

Thakur, A.K., Attri, L., Garg, R.D., Jain, K., Kumar, D., Chowdhury, A., 2024. Temporal and Spatial Dynamics of Subsidence in Eastern Jharia, India, in: ISPRS Annals of the Photogrammetry, Remote Sensing and Spatial Information Sciences. Copernicus Publications Göttingen, Germany, pp. 349–356.

Thakur, A.K., Garg, R.D., Jain, K., 2025. An Assessment of Different Line-of-Sight and Ground Velocity Distributions for a Comprehensive Understanding of Ground Deformation Patterns in East Jharia Coalfield. Remote Sens. Appl. Soc. Environ. 101446.

Thomas, M., 2013. Supplementary cementing materials in concrete. CRC press.

Vanama, V.S.K., Mandal, D., Rao, Y.S., 2020. GEE4FLOOD: rapid mapping of flood areas using temporal Sentinel-1 SAR images with Google Earth Engine cloud platform. J. Appl. Remote Sens. 14, 34505.

Verma, D., Vijay, S., 2024. Time-Series Analysis of Dam Deformation Using Satellite-Based InSAR Technique: Case Studies from Oroville, Pong, and Tehri Dams, in: IGARSS 2024-2024 IEEE International Geoscience and Remote Sensing Symposium. IEEE, pp. 11136–11140.

Vicente, M.A., González, D.C., Mínguez, J., 2019. Recent advances in the use of computed tomography in concrete technology and other engineering fields. Micron 118, 22–34.

Washer, G., Fuchs, P., Graybeal, B.A., Hartmann, J.L., 2004. Ultrasonic testing of reactive powder concrete. IEEE Trans. Ultrason. Ferroelectr. Freq. Control 51, 193–201.

Ye, C.M., Cui, P., Pirasteh, S., Li, J., Li, Y., 2017. Experimental approach for identifying building surface materials based on hyperspectral remote sensing imagery. J. Zhejiang Univ. A 18, 984–990.